Journal of Magnetic Resonance 252 (2015) 120–129

Contents lists available at ScienceDirect

Journal of Magnetic Resonance

journal homepage: www.elsevier.com/locate/jmr

Sample convection in liquid-state NMR: Why it is always with us, and what we can do about it

I. Swan [a], M. Reid [b], P.W.A. Howe [b], M.A. Connell [a], M. Nilsson [a], M.A. Moore [c], G.A. Morris [a,*]

[a] School of Chemistry, University of Manchester, Oxford Road, Manchester M13 9PL, UK
[b] Syngenta, Jealott's Hill Research Centre, Bracknell RG42 6EY, UK
[c] School of Physics and Astronomy, University of Manchester, Oxford Road, Manchester M13 9PL, UK

ARTICLE INFO

Article history:
Received 22 November 2014
Available online 27 December 2014

Keywords:
Convection
Diffusion
DOSY

ABSTRACT

Many NMR experiments on liquids suffer if the sample convects. This is particularly true for applications, such as the measurement of diffusion, that rely on spatial labelling of spins. It is widely assumed that, in most well-conducted experiments with stable temperature regulation, samples do not convect. Unfortunately this is not the case. It is shown here that typical NMR samples show measurable convective flow for all but a very narrow range of temperatures; convection is seen both above and below this range, which can be as small as a degree or so for a mobile solvent such as chloroform. This convection is driven by both vertical and horizontal temperature gradients.

Measurements of convection velocity are presented for a range of samples, sample tubes, probes, and temperatures. Both decreasing sample tube inner diameter and changing sample tube material from glass to sapphire can slow convection markedly, with sapphire tubes being particularly effective. Such tubes are likely to be particularly helpful for accurate measurement of diffusion by NMR.

1. Introduction

All NMR experiments in the liquid state are potentially vulnerable to disturbance if the liquid is in motion. This vulnerability is at its greatest in the many experiments that use field gradient pulses, whether to enforce coherence transfer pathways, to encode spatial position, or to allow diffusion measurement. Where temperature gradients across the sample lead to convection, experiments can show severe signal anomalies in both amplitude and phase. This leads to problems such as signal loss (particularly important in multidimensional NMR experiments), and overestimation of diffusion coefficients in diffusion measurements.

At first sight, the problem of convection should be straightforward to avoid. Convection, in its most familiar form, arises when a sample of liquid is warmer at its base than its top [1]: the warmer, less dense liquid rises, and the colder, denser liquid sinks. This is known as Rayleigh–Bénard convection, and, importantly, is a critical phenomenon: convection only starts when the negative vertical temperature gradient, $-dT/dz$, reaches a certain critical value determined *inter alia* by the sample geometry and by the dynamic viscosity, thermal diffusivity and thermal expansion coefficient of the liquid. In particular, such convection cannot happen where the liquid temperature increases with height (i.e. where the top of the sample is warmer than the bottom). In most probes in superconducting spectrometers, sample temperature is controlled by passing gas of regulated temperature from a variable temperature ('VT') controller upwards past the vertical sample tube, exiting past the sample turbine. Since the base of the NMR tube is the first part that the incoming air encounters, the vertical temperature gradient within the sample should be *positive* (top warmer than bottom) whenever the temperature of the incoming gas is below the quiescent temperature, T_Q, of the sample (the temperature, usually around room temperature, that it would reach in the absence of the VT gas flow), and *negative* when the VT temperature is above T_Q.

It would therefore be reasonable to expect – and indeed is commonly assumed – that the liquid in an NMR tube should remain static, not convecting, whenever the VT is set below room temperature, and for some way above this (until the vertical temperature gradient is sufficiently negative for Rayleigh–Bénard convection to begin). Unfortunately this is not true in practice: as the measurements reported here show, convection occurs at nominal temperatures both above and below room temperature. The reason is that neither the probe geometry nor the incoming VT gas flow is cylindrically symmetric, so small horizontal temperature gradients arise across the sample. Such gradients also drive convection, known as Hadley convection or Hadley flow [1]; this is of major

* Corresponding author.
E-mail address: g.a.morris@manchester.ac.uk (G.A. Morris).

http://dx.doi.org/10.1016/j.jmr.2014.12.006
1090-7807/

importance, for example, in determining global weather patterns. Crucially, horizontally-driven convection is not a critical phenomenon, and does not cease below some critical value of horizontal temperature gradient [1,2]. The unwelcome practical consequence is that Hadley convection is present to a greater or lesser extent in all NMR experiments on liquids: the best that can be achieved is to minimise the rate of such convection.

The presence of horizontal temperature gradients in NMR samples has been demonstrated several times [3,4]. However, with one important exception [5] (and a cursory mention in an earlier paper [6]), the role of horizontal temperature gradients in causing convective flow in NMR experiments seems to have escaped attention in the literature, and even in Chung et al., [5] the ability of horizontal gradients *alone* to cause convection is not fully recognised. Even the presence of convection itself in low temperature NMR experiments [7] seems to have been little remarked upon (although at least one other observation of convection under a positive vertical temperature gradient has been reported [3]).

Temperature gradients arise in NMR probes primarily as a consequence of attempts to control sample temperature by passing temperature-regulated gas past the sample. If all gas flow to a probe is cut off (where it is safe to do so – this is *not* the case for 'cryoprobes'/'cold probes') and the sample is allowed to equilibrate to its quiescent temperature T_Q, the sample temperature is usually found to be very uniform (this is unlikely to be so in the more extreme thermal environment of a cold probe, where T_Q may be far below room temperature). Whenever temperature-controlled gas (VT gas) is used, the internal construction of the probe and the heat flow paths into and out of the sample conspire to generate both horizontal and vertical temperature gradients, and convection ensues to a greater or lesser extent.

Two types of strategy are commonly used to deal with the problem of convection: either to choose experimental conditions (e.g. sample geometry) that minimise the rate of convection, or to use pulse sequences that are designed to compensate for the effects of flow on the signals measured. The two strategies are not mutually exclusive; indeed at extremes of temperature, neither would be sufficient on its own. Methods for reducing the rate of convection include the use of narrower sample tubes [5,8] (with or without thicker walls); sample spinning [9,10] (which *inter alia* reduces the effective size of the convection cell by adding a centrifugal force to the effect of gravity, making the sample convect at an angle to the vertical); reducing sample length with e.g. a Shigemi tube [5,11] (although here it is unclear whether the reduced sample height or the improved heat conduction above and below the active volume given by the solid glass components provides the greater benefit); and using concentric sample tubes [4,7,11]. Since gravity acts vertically, most convective flow is vertical and hence experiments using horizontal rather than vertical field gradient pulses can be much less susceptible to convective flow. This is not a complete answer, however, since pulsed field gradients are spatially non-uniform [12] and vertical flow will take spins through different magnitudes of horizontal field gradient, slightly degrading refocusing. A very simple way to minimise convection in samples where good spectral resolution is not required is to pack the sample with glass wool [13].

Convection-compensated pulse sequences for diffusion measurement [6,14–21] are typically designed to refocus the effects of a constant velocity of flow along a field gradient direction, usually by splitting the diffusion weighting sequence element into two symmetrical halves generating equal and opposite flow effects, although higher order correction (for acceleration, etc.) is also possible. One alternative use for convection-compensated pulse sequences, exploited here, is for the measurement of convection rates, since by varying the balance between the two halves of a compensated sequence the influence of convection on signal amplitude can be controlled and hence the range of convective flow velocities determined [3]. It is also possible to make spatially-resolved measurements of flow velocities in NMR tubes using MR imaging methods [22,23].

The purpose of this paper is to demonstrate the unexpectedly high incidence of convective flow in typical NMR samples, to quantify the problem, and to illustrate some simple strategies for reducing such flow. Measurements are reported for a variety of different spectrometers, solvents and sample tube types; in particular glass and sapphire tubes are compared, as the much higher thermal conductivity of sapphire can greatly reduce both horizontal and vertical temperature gradients. Convection velocities are reported as a function of nominal sample temperature for different sample/tube/spectrometer combinations. Temperature gradients within the sample increase as the difference between the VT temperature and the quiescent sample temperature increases, resulting in a common pattern of convection velocity increasing either side of T_Q.

2. Theory

The experiments in this paper use the convection-compensated homonuclear 2D *J*-resolved IDOSY sequence [6,18] illustrated in Fig. 1, varying the convection compensation imbalance delay, $\Delta\Delta$, to map out the signal variation caused by sample flow in the direction (z) of the field gradient. Although diffusion is not measured in the experiments described, at each temperature a constant attenuation due to diffusion is present (and the apparent diffusion coefficient could be determined by incrementing the PFG magnitude, adding another experimental dimension). The time interval Δ is commonly referred to as the diffusion delay; this usage will be retained here, although in this context the term 'velocity-encoding delay' would be more appropriate. The sequence of Fig. 1 is designed to cancel the effects of constant flow when the diffusion delay imbalance $\Delta\Delta$ is zero, allowing diffusion-weighted data to be acquired without interference from convection. When $\Delta\Delta$ is non-zero, the signals from species with magnetogyric ratio, γ, moving with constant z velocity v acquire a phase shift $-\gamma\delta G v \Delta\Delta$. Since a convecting NMR sample has equal net upward and downward flows of liquid, the net result of the phase shifts averaged over the sample is an attenuation of the overall signal. The form of signal amplitude attenuation as a function of delay imbalance, $S(\Delta\Delta)$, will depend on the velocity spectrum $M(v)$, the relative amount of signal as a function of vertical flow velocity v:

$$S(\Delta\Delta) = \int_{-\infty}^{\infty} M(v)\exp(-i\gamma G v \delta \Delta\Delta)\mathrm{d}v \Big/ \int_{-\infty}^{\infty} M(v)\mathrm{d}v \tag{1}$$

In an ideal probe $S(\Delta\Delta)$ will be real, but can be negative (the first moment of $M(v)$ must be zero if the sample is to remain in the tube, so if the spatial variations of M and G are uncorrelated the integral is real). The velocity spectrum can be calculated from the spatial distribution of velocity $v(r, \phi)$ in cylindrical coordinates:

$$M(v') = LM_{\mathrm{vol}} \int_{-\infty}^{\infty}\int_{0}^{R}\int_{0}^{2\pi} \delta(v - v')v(r, \phi) r\,\mathrm{d}\phi\,\mathrm{d}r\,\mathrm{d}v \tag{2}$$

where M_{vol} is the signal per unit volume, L the length of the active sample volume and δ the Dirac delta function. The additional attenuation due to diffusion is independent of $\Delta\Delta$, and is given by the usual Stejskal–Tanner equation [24].

The theoretical form of the laminar velocity distribution for convection in an infinitely long vertical cylinder, driven by a purely vertical temperature gradient, is given [2,22] by

$$v(r, \phi) = \sum_{n=0}^{\infty} v_n \left(\frac{I_n(kr)}{I_n(kR)} - \frac{J_n(kr)}{J_n(kR)}\right)\cos n\phi \tag{3}$$

where the v_n are system-dependent constants, r is the radial and ϕ the angular coordinate, R is the cylinder's internal radius, k is

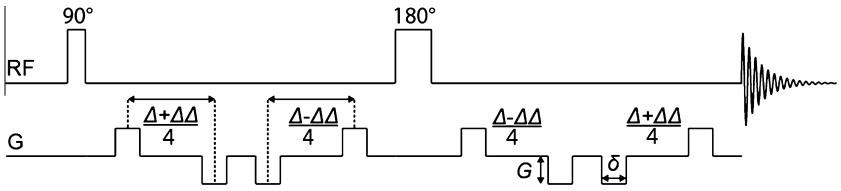

Fig. 1. Pulse sequence used. Each gradient pulse is of duration is δ, the total diffusion time is Δ and the delay imbalance is $\Delta\Delta$. The effects of constant laminar flow on signal amplitude are cancelled when the $\Delta\Delta$ is zero; varying $\Delta\Delta$ systematically allows the effect of convection on signal amplitude to be mapped out and convection velocity distribution to be determined.

related to the Rayleigh number, *Ra*, for the system, and J_n and I_n are the Bessel and modified Bessel functions of the first kind respectively. For this geometry, v_n is only non-zero for odd values of n, and is greater for low values of n. The constant k is equal to $Ra^{-1/4}/R$, where the Rayleigh number, *Ra*, is given by

$$Ra = -\frac{g\beta\rho^2 c_p R^4 \frac{dT}{dz}}{\eta\kappa} \tag{4}$$

where g is the acceleration due to gravity in m s^{-2}, β is the volumetric thermal expansion coefficient in K^{-1}, ρ is the fluid density in kg m^{-3}, c_p is the specific heat capacity in J kg^{-1} K^{-1}, dT/dz is the vertical temperature gradient in K m^{-1}, η is the dynamic viscosity in Pa s and κ is the thermal conductivity in W m^{-1} K^{-1}. Under the conditions of typical NMR experiments, flow is indeed laminar and $n = 1$ [22]. As noted earlier, convection driven by a purely vertical temperature gradient (Rayleigh–Bénard convection) is a critical phenomenon. Convection will only occur when the temperature gradient $-$dT/dz is sufficiently high for the Rayleigh number *Ra* to exceed a critical value, here 67.4 and 215.8 for insulating and perfectly conducting surrounding media, respectively [22]. For chloroform in a standard (thin-walled) 5 mm NMR tube, a vertical temperature gradient of magnitude less than 0.3 K cm^{-1} is sufficient to cause convection, whereas water would require about 6 K cm^{-1}. However, as the results presented below demonstrate, in typical NMR experiments pure vertical temperature gradients are simply not seen: in all the systems studied here, convection was observed at temperature gradients well below the critical Rayleigh–Bénard threshold, indicating the presence of horizontal temperature gradients.

In the case of a purely horizontal temperature gradient, here arbitrarily chosen to lie in the x direction, the laminar flow shape derived by Ostroumov (obtained by rearrangement of equations 5.18 in Ref. [2]) has the same form as that for vertical convection with low Rayleigh number and $n = 1$

$$v(r,\phi) = \frac{dT}{dx}\frac{R^3 g\beta\rho}{4\eta(1+\kappa/\kappa_e)}\left(\frac{r}{R}\right)\left[1-\left(\frac{r}{R}\right)^2\right]\cos\phi \tag{5}$$

where dT/dx is the transverse temperature gradient in K m^{-1}, ρ is the density in kg m^{-3}, κ_e is the effective thermal conductivity of the medium surrounding the vertical cylinder, and other symbols have the same meanings as previously. The angular dependence and velocity spectrum for such a flow are shown in Fig. 2. (Note that the term in κ/κ_e arises from the assumption that there are no local heat sinks or sources outside the cylinder; this is not the case for an NMR sample, where the effect of the exchange of heat with the flow of VT gas can be approximated by setting κ_e equal to infinity, as used in Fig. 2). Analytical forms for the signal dependence on $\Delta\Delta$ (Eq. (A7)) and the velocity spectrum (Eq. (A13)) are derived in the Appendix A.

The velocity spectrum of Fig. 2b is bounded by a velocity $\pm v_{max}$, which depends on the convecting system. The spectrum shows a cusp at zero velocity, as a consequence of the requirement that the vertical velocity go to zero at the periphery of the sample and in the medial nodal plane. In practice, experimentally measured velocity spectra show a less pronounced central feature [3], possibly reflecting horizontal temperature gradients that are nonlinear and have different directions and magnitudes at different heights within the sample. (Twists in 3D velocity distributions have been reported in experimental measurements on NMR samples [22].) For a vertical temperature gradient, v_{max} has a complicated dependence on the sample geometry, material properties and Rayleigh number, but for a horizontal temperature gradient in a conducting tube it is given by

$$v_{max} = \frac{R^3 g\beta\rho}{\sqrt{108}\eta}\frac{dT}{dx} = \chi\frac{R^3 g}{\sqrt{108}}\frac{dT}{dx} \tag{6}$$

where the quantity $\chi = \beta\rho\eta$ is a measure of the ease with which a sample of a given liquid convects under a horizontal temperature gradient. The quantity χ and the ratio of χ to that for chloroform are tabulated for the protio forms of some common NMR solvents and for D_2O in Table 1. It is noteworthy that water and D_2O are far less prone to convection than solvents such as chloroform and methanol. It is common to attribute this to their higher viscosity, but in fact it is the lower coefficient of thermal expansion, a consequence of the increasing breakdown of hydrogen bonding structure in water with temperature, that has the biggest effect.

As stated previously, there are two common ways of minimising the effects of convection in NMR experimental results: the first is to suppress or reduce the convective flow itself, and the second is to refocus the effects due to flow during an experiment. The pulse sequence in Fig. 1 with $\Delta\Delta = 0$ does the latter, as do many other sequences [4,16,17,21,25]. The former can be accomplished in a number of ways, by controlling how heat flows into, out of, and across the sample.

One simple solution mentioned in the introduction can be to spin the sample, relatively slowly. While the benefits of spinning have been attributed to the Coriolis effect [9], the effect of centrifugal force in changing the direction of convection and hence constraining its geometry seems a more likely candidate, and the results below suggest that the dominant effect may in fact be the very effective averaging of transverse temperature gradients that spinning accomplishes. The problems with spinning are that it generates mechanical instabilities, and that unless scrupulous care is taken to synchronise the timing of gradient pulses with the sample rotation, small spatial inhomogeneities in the gradient field will lead to large signal disturbances. For these reasons sample spinning is not recommended for accurate diffusion measurements.

A common approach to reducing temperature gradients is to increase the rate of flow of the VT gas. Unfortunately this again is limited in its utility, because too high a gas flow will lead to vibration in the probe, sometimes compounded by 'organ pipe' acoustic resonances in the upper barrel of the magnet. A much more effective way to reduce convection, and in the case of vertical temperature gradients to delay its onset, is to constrain the sample geometry. As Eqs. (4) and (6) show, convection in a vertical cylinder is governed by functions of third and fourth order in tube internal diameter, and constraining the height of a sample can also slow

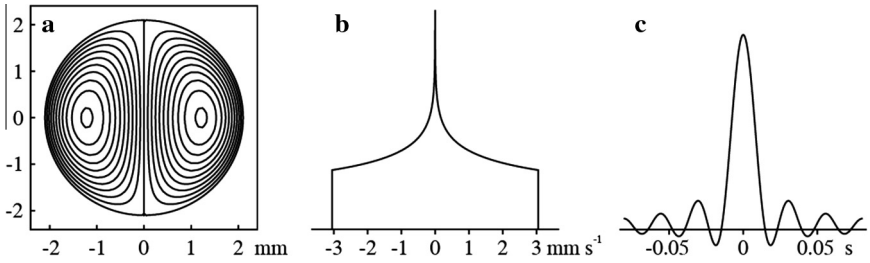

Fig. 2. (a) Calculated spatial dependence (Eq. (5)) of vertical convective flow velocity (contour spacing 0.3 mm s^{-1}), (b) velocity spectrum $M(v)$ (Eq. (A13)), and (c) signal dependence on timing imbalance $\Delta\Delta$ (Eq. (A7)) for a standard (thin-walled) 5 mm NMR tube of 4.2 mm ID containing chloroform at 25 °C in the presence of a 0.5 K cm^{-1} horizontal temperature gradient, assuming a perfectly conducting tube wall.

Table 1
Physical parameters determining the rate of convection driven by a horizontal temperature gradient for protio forms of common solvents at 25 °C.

	Chloroform	DMSO	H_2O	D_2O	Acetone	Methanol	Toluene
$\beta/(10^{-3}\ K^{-1})$	1.27	0.942	0.257	0.172	1.43	1.49	1.08
$\rho/(10^3\ kg\ m^{-3})$	1.489	1.0955	0.997	1.044	0.791	0.791	0.865
$\eta/(10^{-3}\ Pa\ s)$	0.542	1.991	0.890	1.095	0.315	0.544	0.56
$\chi/(10^3\ s\ K^{-1}\ m^{-2})$	3.49	0.518	0.280	0.174	3.59	2.17	1.67
$\chi/\chi_{chloroform}$	(1)	0.15	0.080	0.050	1.03	0.62	0.48

convection. A relatively small decrease in sample size can cause a big reduction in convection, as illustrated in some of the results below.

A very effective way to reduce sample temperature gradients is to increase the efficiency of heat transfer within the sample tube walls. Using thicker glass will give a small improvement, but changing the tube material from glass to sapphire has a much larger effect. The thermal conductivity of sapphire is approximately 25 times that of borosilicate glass [26], so an NMR tube made of sapphire will greatly reduce temperature gradients over the active volume of a sample, particularly in the case of horizontal gradients.

As shown by Eq. (2), the attenuation function $S(\Delta\Delta)$ is proportional to the inverse Fourier transform of the velocity spectrum. While the analytical form of $M(v)$ for Eq. (5) is relatively intractable, the experimental form of the velocity spectrum is, as noted by Loening and Keeler [3], quite well approximated by a top hat function. Experimental attenuation functions are therefore intermediate in form between that of Fig. 2c and a sinc function, and by fitting experimental data for signal attenuation as a function of $\Delta\Delta$ to a sinc function it is possible to obtain good estimates of the width of the velocity spectrum and hence of v_{max} [3].

3. Experimental

Of the solvents in common use for NMR, one of the most susceptible to convection is chloroform. A 5 cm deep solution of $CHCl_3$, 5% v/v, doped to decrease T_1 with $Cr(acac)_3$, 0.2 mg ml^{-1}, in $CDCl_3$ was therefore chosen for an investigation into convection rates as a function of nominal probe temperature (the temperature at which the variable temperature controller is set to regulate) for different types of sample tube. Two shorter series of experiments were then performed, using firstly, a sample of residual HDO in D_2O, to show the effect of using a less mobile solvent, and secondly, a chloroform sample in a thin-walled glass 3 mm NMR tube, to show the effect of reducing sample outer diameter. Of the five types of NMR sample tube used, three had glass walls, with a specified outer diameter (OD) of 4.97 ± 0.013 mm and inner diameters (ID) of 4.20, 3.43 and 2.20 ± 0.025 mm respectively; these will be referred to henceforth as standard, medium-walled and thick-walled tubes, respectively. A fourth glass tube had an OD of 2.99 ± 0.01 mm and an ID of 2.42 ± 0.01 mm. As the majority of NMR tubes are made with thin glass walls, these four tubes are of the greatest practical interest. The fifth tube was made of crystalline sapphire and had nominal OD 5.00 ± 0.13 mm and ID 3.48 ± 0.23 mm (see Table 2).

NMR experiments were conducted using three spectrometers:

(1) A Varian VNMRS 500 spectrometer equipped with a 5 mm triple resonance probe and a triple-axis PFG coil giving a maximum z gradient of 68 G cm^{-1}. Individual rectangular z gradient pulses of nominal amplitude 31 G cm^{-1} and duration 1 ms were used throughout the sequence. Dry air was used for the VT gas, at a flow rate of 9 L min^{-1}, using the manufacturer's standard temperature regulation with precooling of the input air pipe by solid CO_2 pellets.
(2) A Varian INOVA 400 spectrometer equipped with a 5 mm dual probe and a z-axis PFG coil giving a maximum nominal gradient of 32 G cm^{-1}. Individual PFG pulses of rectangular amplitude 31 G cm^{-1} and duration 1 ms were used throughout the sequence. VT air at 9 L min^{-1} was temperature regulated as in above.
(3) A Bruker DRX 500 spectrometer equipped with a 5 mm broadband inverse dual probe and a z axis PFG coil giving a maximum nominal gradient of 54 G cm^{-1}. Individual half-sine gradient pulses of maximum amplitude 49 G cm^{-1} and duration 1 ms were used throughout the sequence. Dry air was used for the VT gas, at a flow rate of 9 L min^{-1}, using the manufacturer's standard temperature regulation with precooling of the input air by a BCU-05 refrigeration unit.

The experiments used the pulse sequence of Fig. 1 with a total diffusion delay, Δ, of 0.08 s and 25 different diffusion delay

Table 2
Materials and inner diameters of the five types of NMR tube used in the experiments reported.

Inner diameter (ID) (mm)	Material	Label
4.20 ± 0.025	Glass	Standard
3.43 ± 0.025	Glass	Medium-walled
2.20 ± 0.025	Glass	Thick-walled
2.42 ± 0.01	Glass	3 mm
3.48 ± 0.23	Sapphire	Sapphire

imbalance times, $\Delta\Delta$. The array of values of $\Delta\Delta$ was tailored to sample more densely for small $\Delta\Delta$, in order to ensure that the characteristic features of the sinc dependence of signal on $\Delta\Delta$ could be recorded, and hence an accurate estimate of v_{max} obtained by least squares fitting, for the full range of convection velocities seen in the experiments. At each temperature a stabilisation delay of 15 min was allowed after the nominal temperature was reported by the VT system as having been reached, in order to ensure that the sample was fully equilibrated with its surroundings in the probe. Experimental data were processed with 10 Hz of Lorentzian line broadening, to minimise the effect of any small changes in experimental lineshape, and the phase of each spectrum was adjusted in order to correct for the effects of lock disturbance by the field gradient pulses. (The appropriate zeroth order phase correction as a function of $\Delta\Delta$ for each set of experiments was determined by examining the data for the temperature showing the slowest convection, then applying the same correction to the data for all the other temperatures studied.)

The experimental signal amplitude data thus obtained were then subjected to nonlinear least squares fitting using MS Excel's GRG non-linear fitting engine with the function

$$F(\Delta\Delta) = S_0 \sin(\gamma\delta G A_G v_{max}\Delta\Delta)/(\gamma\delta G A_G v_{max}\Delta\Delta) \quad (7)$$

where S_0 is the maximum signal amplitude and A_G the gradient pulse shape factor (1 for rectangular pulses, on instruments 1 and 2, and $2/\pi$ for half-sine pulses, on instrument 3) in order to determine v_{max}. (In contrast to the corresponding calculation for diffusional attenuation, using half-sine shaped rather than rectangular gradient pulses only requires the inclusion of the shape factor A_G, to allow for the difference in gradient pulse area, and does not require a gradient pulse shape-dependent correction to Δ to allow for the effects of motion during the gradient pulses).

Direct measurements of temperatures inside a standard (thin-walled) 5 mm NMR tube were carried out in a bench rig consisting of a thermally insulated Varian 500 MHz ^{1}H probe and upper barrel assembly, connected to an Oxford Instruments VTC4 variable temperature controller and supplied with nitrogen gas. A standard 5 mm NMR tube was fitted with NTC thermistors (Farnell Components type 353-2409), of dimension 0.5 × 0.5 × 1 mm, fixed to the inside with epoxy resin at heights above the inside of the tube base of 0.5, 16, 34, 52, 72, 112 and 178 mm. The thermistors were connected to measurement electronics (an 8 channel ADC, Measurement Computing type PMD-1608FS, connected to a PC) using 0.08 mm/46 s.w.g. constantan wire to minimise unwanted heat flow. After calibration of the individual thermistor characteristics, the tube was fitted as normal into a 5 mm ID turbine and lowered into the rig to rest in the air bearing of the upper barrel, so that the thermistors were below, inside, and above the active volume of the probe. The probe temperature was regulated at a nominal 50 °C using an air flow rate of 10 L min^{-1}, and with the aid of an improvised goniometer the angular dependence of the inner tube wall temperature was mapped for the lowest four of the seven thermistor sites.

4. Results and discussion

Representative results for signal attenuation as a function of delay imbalance $S(\Delta\Delta)$ are shown in Fig. 3, for experiments in standard tubes at the highest and lowest temperatures studied. The results of iterative fitting confirm that the experimental attenuation functions, and hence the velocity spectra, lie between the analytical forms derived in the Appendix A (Eq. (A7)) and the simple approximation (Eq. (7), rectangular velocity spectrum) used in Ref. [3]. The maximum convection velocities v_{max} yielded by the two fitting methods differ only slightly, Eq. (A7) giving values

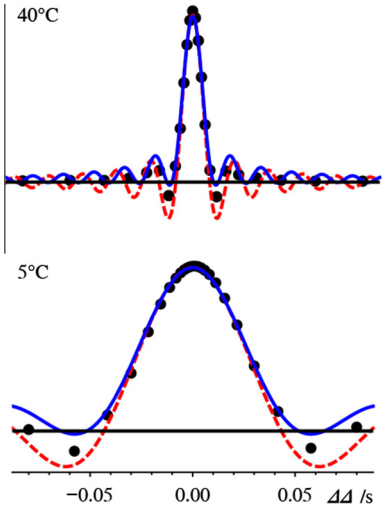

Fig. 3. Experimental measurements of $S(\Delta\Delta)$ (black dots) and fits to Eq. (7) (red dashed line) and A7 (blue solid line), for measurements in standard tubes at 40 °C (top) and 5 °C (bottom) in spectrometer system 2. (For interpretation of the references to colour in this Figure legend, the reader is referred to the web version of this article.)

about 10% greater in each case, so the simpler of the two fitting methods, that of Eq. (7), was applied to all of the experimental data.

The leftmost three plots in Fig. 4 show the maximum rates of convection v_{max} obtained for chloroform samples in the standard, medium-walled and thick-walled tubes and in the sapphire tube, on a Varian 400 MHz, Varian 500 MHz and Bruker 500 MHz spectrometer respectively, at 1 °C intervals from 5 °C to 40 °C. The rightmost plot compares a chloroform sample in the 3 mm tube, and a D_2O sample in the standard tube, against the chloroform data for the thick-walled and sapphire tubes on the Varian 400 MHz spectrometer. Rates were determined by iterative fitting to Eq. (7), as described earlier.

A number of things are immediately apparent. First, all the samples in all the spectrometers studied showed evidence of convection both at temperatures above T_Q and at temperatures below T_Q: only very close to T_Q was convection too slow to be detected with the experimental parameters used. Second, rates of convection rose more steeply with temperature difference from T_Q for temperatures above T_Q, where both horizontal and vertical temperature gradients can drive convection, than below, where only horizontal gradients should contribute. Third, the effect of reducing sample tube ID was, as expected, to reduce convection rate markedly. Fourth, again as expected, the use of a sapphire tube greatly reduced convection compared to a standard tube under all the conditions studied, and showed the lowest rate of convection of any of the 5 mm tubes under all conditions except at the top end of the range of temperatures studied (above 38 °C in spectrometers 1 and 3 and above 35 °C in spectrometer 2). In the light of the theory presented earlier, the significance of the "V" shape of the curves of v_{max} versus temperature is clear. The rate of horizontally-driven convection is directly proportional to the horizontal temperature gradient, and only touches zero where the gradient is zero and both the sign of the temperature gradient and the direction of convection change sign; a plot of convection velocity at a point to one side of the tube would show a simple straight line passing through zero.

Using a 3 mm tube and changing the solvent to D_2O both reduced convection rates very substantially. The results of experiments on a chloroform sample in a 3 mm tube, and on a D_2O sample in a standard tube, are compared in Fig. 4d with the data from

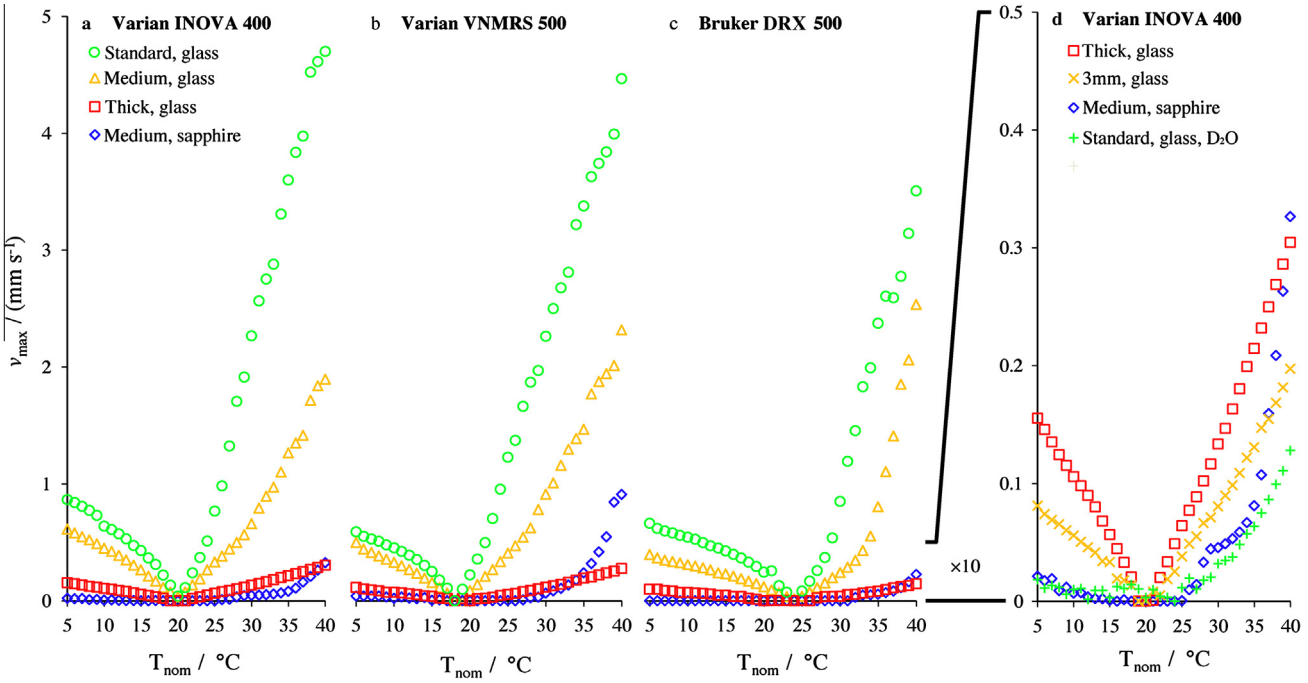

Fig. 4. Plot of maximum convection velocity, v_{max}, as a function of nominal VT, T_{nom}, on (a) and (d) a Varian INOVA 400 MHz, (b) a Varian VNMRS 500, and (c) a Bruker DRX 500 MHz spectrometer, for different 5 mm NMR tubes (green circles for a standard tube, ID 4.20 mm; orange triangles for a medium-walled tube, ID 3.43 mm; red squares for a thick-walled tube, ID 2.20 mm; and blue diamonds for a sapphire tube, ID 3.48 mm). (d) Compares, on an expanded velocity scale, the results of changing the NMR tube OD to 3 mm (orange saltire crosses) or solvent to D_2O in a standard tube (green ordinary crosses), on the Varian INOVA 400 MHz spectrometer, with those for thick-walled and sapphire tubes. (For interpretation of the references to colour in this figure legend, the reader is referred to the web version of this article.)

Fig. 4a for chloroform in thick-walled and sapphire tubes. The 3 mm tube has a marginally larger ID (2.42 ± 0.007 mm), but much smaller OD (2.99 ± 0.007 mm), than the thick-walled tube and shows significantly less convection. This suggests that allowing the VT air to circulate more freely around the tube (as a consequence of the increased air gap between tube and insert) is more effective at reducing horizontal temperature gradients than maintaining the same clearance and using a thicker wall to increase thermal conduction through the glass. As expected, changing from $CDCl_3$ to D_2O drastically reduces the rate of convection. The effect is even greater than that predicted from the values in Table 1, but it should be borne in mind that the theoretical predictions assume a uniform horizontal temperature gradient and that the gradients seen experimentally will depend on the sample as well as the environment in which it sits, complicating comparisons.

The data for the behaviour of convection in the sapphire tube are worthy of special comment. At temperatures below T_Q, in the range 5 °C to approximately 20 °C, convection in the sapphire tube remains very slow in all of the experiments performed. Above T_Q, convection rates rise first slowly and then more rapidly, overtaking those seen for the thick-walled tube in the range 35–40 °C. It is tempting to attribute the sudden rise in convection rate to the critical onset of Rayleigh–Bénard convection, but this is almost certainly incorrect. Convection driven by a mixed (as opposed to uniaxial) gradient is unlikely to be well approximated by some combination of the behaviours seen for pure horizontal and vertical gradients; rather, the symmetry breaking caused by a horizontal gradient is likely to lead to an earlier onset of Rayleigh–Bénard convection (as has been noted experimentally in NMR samples [27]). An alternative explanation for this change in behaviour could be the increased influence of the heat reservoir attached to the upper part of the NMR tube. The thermal contact between the turbine holding the NMR tube and the air bearing that supports the turbine, and that between the turbine and the NMR tube, will lead to a vertical temperature gradient in the tube that is partly determined by the thermal conductivity of the tube material and by the temperature difference between sample active volume and turbine. For temperatures close to T_Q, vertical temperature gradients at the active volume caused by temperature gradients within the probe components are likely to dominate, but at temperatures far from T_Q the heat flow along the tube to or from the turbine will come to dominate. In the case of a glass tube, the relatively low thermal conductivity that allows horizontal temperature gradients to cause such mayhem works to delay the onset of vertical gradients caused by heat exchange with the turbine. In the case of a sapphire tube the much more efficient thermal conduction has the opposite effect, reducing horizontal gradients but lowering the temperature differential at which heat exchange with the turbine becomes a problem. One consequence is that the advantages of a sapphire tube may be lost at high temperatures if the sample tube is not insulated from its surroundings.

The direct measurements of internal temperatures within a standard tube fitted with thermistors at a nominal sample temperature of 50 °C allowed order of magnitude estimates to be made of the convection rates to be expected in chloroform. The measurements showed angular variations in internal temperature that varied from 0.35 to 1.3 K peak-to-peak, with the largest variation being at the base of the tube. The magnitudes of the horizontal temperature gradients were 0.31, 0.17, 0.08 and 0.2 K mm^{-1} for the sensors 0.5, 16, 34 and 52 mm above the base of the tube respectively, with the axes of the gradients at the three uppermost sensors shifted by approximately 80°, 90° and −40° respectively with respect to that at the lowest sensor. Fig. 5 shows the disposition of the thermistors and the angular dependence of the measured temperatures. Assuming that the temperature gradients are directly proportional to the deviation from quiescent temperature, the average gradients within the probe active volume (bracketed by the second and third sensors) in this assembly at 5 and 40 °C would then be approximately 0.07 and 0.09 K mm^{-1}.

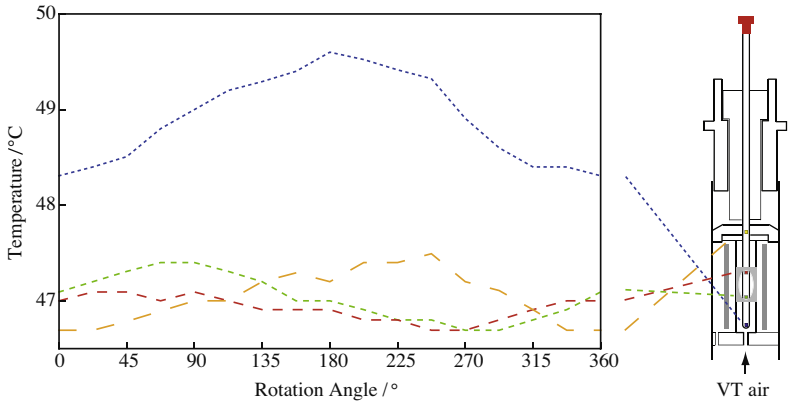

Fig. 5. Angular dependence of temperatures measured using thermistors mounted within a standard 5 mm NMR tube, and schematic illustration of the disposition of the thermistors within the tube and probe. The temperatures shown are for the sensors mounted 0.5, 16, 34 and 52 mm above the base of the tube (blue, green, red and yellow, respectively with increasing length of dashed line), at a nominal regulated sample temperature of 50 °C. (For interpretation of the references to colour in this figure legend, the reader is referred to the web version of this article.)

In a tube containing chloroform, such gradients would (Eq. (6)) give maximum convection rates of 2.1 and 2.7 mm s^{-1} respectively. The system on which the temperature gradient measurements were made differs materially from those in which experiments were performed – the probe was of slightly different construction from those used in spectrometers 1 and 2, and quite different from that of spectrometer 3, the bench rig was not inside the buffering thermal environment of a magnet, and most importantly the NMR tube fitted with thermistors did not contain any liquid to moderate the temperature gradients – but it is still interesting to compare these values with the experimental values measured at 5 °C and 40 °C on system 1 (0.9 and 4.6 mm s^{-1} respectively) and 2 (0.6 and 4.5 mm s^{-1} respectively). As expected, the values of v_{max} measured at low temperature are smaller than those predicted for an empty tube in a bench rig: the thermal contact with the magnet, and more importantly the heat transfer by the liquid in the experimental tube, should significantly reduce the experimental transverse temperature gradient. For temperatures above T_Q, the same argument does apply, but, as the much greater experimental rate of change of v_{max} with temperature above T_Q shows, the added effect of vertical temperature gradients needs to be taken into account. The general agreement in order of magnitude between prediction and experiment here is comforting given the major uncertainties involved, and confirms that there is no major discrepancy in convection rates between those measured experimentally and order of magnitude estimates based on bench-measured temperature gradients.

The stark observation that significant convection is present under almost all experimental conditions was unexpected, but in the light of the known theory summarised here should not have been. The practical implication is that almost all diffusion measurements made using uncompensated sequences are vulnerable to error. Convection compensation is, unfortunately, not a panacea: the greater number of gradient pulses required leads to more field disturbance and greater systematic errors, and generally exacts at least a twofold penalty in signal-to-noise ratio. An effective, pragmatic approach is to perform a quick check for convection using the pulse sequence of Fig. 1 and comparing the signal obtained with $\Delta\Delta = 0$ and $\Delta\Delta > 0$ to see whether convectional attenuation is detectable. If it is not, a conventional pulse sequence can be used; if it is, either the sample conditions need to be changed or a convection-compensated sequence needs to be used. (Where diffusion accuracy is not critical, as for example in qualitative applications of diffusion-ordered spectroscopy, a simpler way to check for convection is to include a very slowly-diffusing reference material such as a high molecular weight polydimethylsiloxane in the sample; any convection will show up as an apparent increase in *D*.) If the exact sample temperature is not critical, cutting off the VT gas supply to the probe (in room temperature probes only, *not* in cold probes) can often reduce convection to a minimum. The probe quiescent temperature can often be manipulated a little by changing the flow rate of cooling/buffering air supplies to probe and/or shims. (*In extremis*, the temperature of the shim coil assembly and hence of the probe it surrounds can be manipulated by changing the choice of shim settings; similar field homogeneity can typically be obtained using radically different settings of shim currents and hence of power dissipation.) It will often be more effective to use a smaller sample than to use a convection-compensated sequence, because commonly-used compensated sequences that use stimulated echoes immediately sacrifice more than half of the available signal, and require very extensive phase cycling for the cleanest results.

If it is necessary to reduce convection but essential to maintain temperature control, a compromise is needed between the degree of reduction of v_{max} and the price in sensitivity. Table 3 shows the relative signal (at constant concentration) calculated from the

Table 3
Average maximum convection velocities, above and below quiescent temperature, and signal intensities for equal sample concentration, relative to those for a standard tube.

Tube type	Maximum relative convection velocity at 5 °C	Maximum relative convection velocity at 40 °C	Relative signal
Standard/thin, glass	1.000	1.000	1.00
Medium, glass	0.646	0.377	0.67
Thick, glass	0.148	0.067	0.27
Medium, sapphire[a]	0.010[a]	0.022[a]	0.69
(3 mm tube) thin, glass	0.078	0.036	0.33
(D_2O solvent) thin, glass	0.020	0.016	1.00

[a] Maximum convection velocities measured in the sapphire tube varied non-linearly with temperature: significantly better reduction in v_{max} was found closer to T_Q.

sample active volume and the maximum relative convection velocity, measured above and below quiescent temperature, at 5 and 40 °C, for different tube types on the Varian 400 instrument used. Figures are normalised to those for the standard tube.

From Table 3, it is apparent that a 3 mm tube is preferable to a thick-walled tube, as the maximum convection velocity is halved and its active volume contains 20% more sample. As noted above, the smaller temperature gradients reflect improved VT air circulation. Where permissible, a change of solvent can greatly reduce convection. If the solvent cannot be altered, the results clearly show that except at high temperatures a sapphire tube gives the best reduction of convection, but this does not necessarily make it suitable for all experiments. First, the sapphire wall is crystalline (not amorphous like glass) and hence magnetically anisotropic, and commercial tubes are not manufactured to the stringent mechanical specifications possible with glass, so magnetic field homogeneity over the active sample volume is typically significantly poorer with sapphire than with glass. Second, sapphire tubes are typically at least an order of magnitude more expensive than conventional glass tubes. Third, as noted above the advantages of the sapphire tube begin to decrease significantly beyond 15 °C above quiescent temperature. Nevertheless, one of the clear messages of the results reported here is that for accurate measurements of diffusion not too far from room temperature and in conventional equipment such as that used here, a sapphire tube is an excellent investment. The next best option of those studied is the 3 mm tube, which halves the signal available but reduces convection velocity tenfold compared with a medium-walled tube. For more extreme conditions, a capillary tube, either in isolation or suspended in a larger tube filled with an NMR-silent (convecting) fluid, may be used.

(It has been assumed implicitly throughout the preceding discussion that convection is a bad thing, but this may not always be the case. Severe convection can lead to signal loss even in standard multidimensional NMR experiments, because it disrupts the refocusing effects of the field gradient pulses used to enforce coherence transfer pathways [15]. However, the majority of such experiments deliberately keep such pulses close in time to minimise losses, and convection is rarely a problem. Disruption of refocusing actually works in favour of such experiments when it comes to the unwanted refocusing of signal from one transient of an experiment to the next [28,29]. Both diffusion and convection thus serve to reduce the impact of rapid pulsing artefacts, and contribute to the common observation that such artefacts are much weaker in 'gradient-enhanced' experiments than in those relying on phase cycling.) Of course, where gradient-enhanced experiments are used far from T_q there is a risk that convection-driven signal attenuation within a given transient will become a problem.

As stated earlier, the effect of even a small amount of convection on diffusion measurements can be significant. To illustrate the practical implications of the convection rates observed in these experiments, Fig. 6 shows the increase in apparent diffusion coefficient seen as a function of maximum convection velocity when typical experiments are simulated with three different diffusion delays Δ for three species with different diffusion coefficients. The conclusions are stark: first, convection with velocities only a few percent of those measured in the experiments of Fig. 4 is sufficient to cause major errors in diffusion coefficient; and second, the statistics of fitting do not reveal any problem until the error in D is very large. The reason for the latter is that, as Fig. 7 illustrates, the distortion of the shape of the signal attenuation curve as a function of gradient amplitude squared, that is caused by convection, only leads to significant deviations from an exponential at high convection velocities. In practice, experimental signal decays already deviate from the theoretical Stejskal–Tanner form even in the absence of convection, because of the spatial non-uniformity of pulsed field gradients [12]. Slow convection leads to faster signal decay, and hence to a greater apparent diffusion coefficient, but has very little effect on the statistical uncertainty of the estimation of that diffusion coefficient. Using the sinc approximation of Eq. (7) for convective signal attenuation, in the small attenuation regime the error D_{est}–D in diffusion coefficient can be approximated by power series expansion as $v_{max}^2\Delta/6$, in agreement with the approximately quadratic dependence on v_{max} seen in Fig. 6.

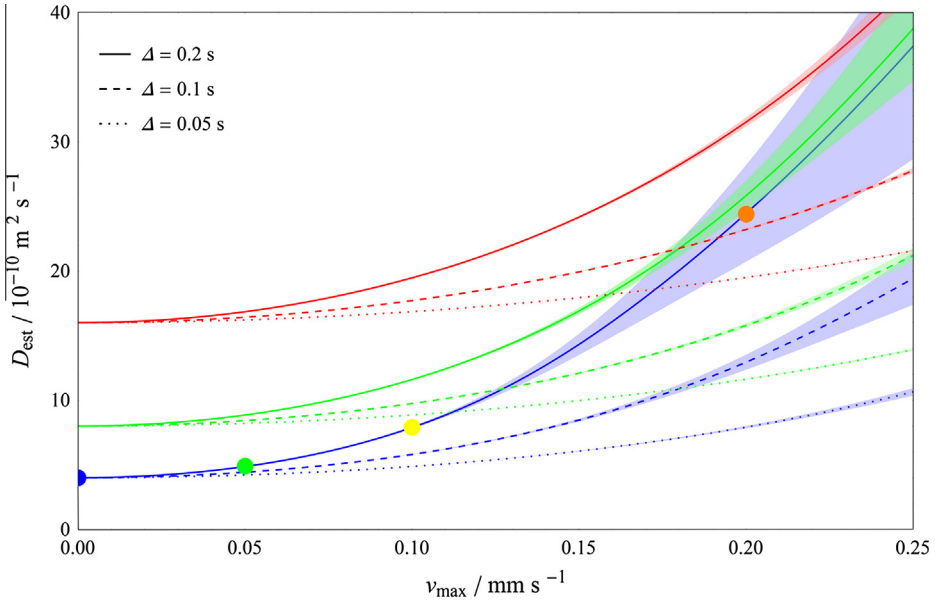

Fig. 6. Estimated diffusion coefficient, $D_{est,}$ (lines) and uncertainty of fit (shaded region, ± standard error) obtained by least squares fitting of calculated signal attenuations for three different actual diffusion coefficients (blue, 4×10^{-10} m^2 s^{-1}; green, 8×10^{-10} m^2 s^{-1}; red, 16×10^{-10} m^2 s^{-1}) as a function of convection velocity. Note the difference in scale from Fig. 4: the convection velocities shown here are much smaller than those actually measured for chloroform. Three different diffusion delays (dotted line, 0.05 s; dashed line, 0.1 s; solid line, 0.2 s) were used, for simulated DOSY experiments using diffusion-encoding gradient pulses with amplitudes varying from 3 to 30 G cm^{-1} in 16 equal increments of gradient squared, and durations tailored to achieve a maximum signal attenuation of e^{-1} in the absence of convection. The filled circles indicate parameters for which the simulated signal measurements and corresponding fitted lines are shown in Fig. 7. (For interpretation of the references to colour in this figure legend, the reader is referred to the web version of this article.)

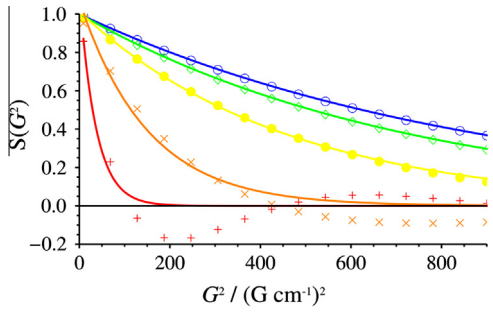

Fig. 7. Estimated exponential fitting (lines) to measurements of signal, S, taken at 16 (marked) equal increments in gradient pulse amplitude squared G^2, for a species diffusing at 4×10^{-10} m^2 s^{-1} in a simulated experiment using gradient pulses of duration 1.4 ms and a diffusion delay Δ of 200 ms, with no convection (blue, empty circles) and maximum convection velocities v_{max} of 0.05 (green, empty diamonds), 0.1 (yellow, filled circles), 0.2 (orange, saltire crosses) and 0.4 (red, ordinary crosses) mm s^{-1}. (For interpretation of the references to colour in this figure legend, the reader is referred to the web version of this article.)

5. Conclusions

Diffusion measurements by NMR are particularly demanding experiments. The velocity-encoding conditions used for the experiments reported here are necessarily (because of the rapid diffusion of $CHCl_3$) very mild; with a slowly-diffusing sample and similar instrumentation it would be relatively straightforward to measure much smaller velocities. Even very slow coherent motions within the active volume along the field gradient axis will have a measurable effect on experimental results. (Like the great majority of instrumental problems, convection tends to increase rather than decrease the apparent diffusion coefficient measured). The longer the diffusion delay is, and the lower the diffusion coefficient being measured, the greater the systematic error that results. Only for relatively rapid convection does the distortion of the signal attenuation function from the expected Stejskal–Tanner form become large enough for the standard error estimated when fitting the signal decay to become noticeable.

One of a number of surprises in the results reported here is the relative similarity of the susceptibility to convection of three different probes with quite different internal constructions. It might have been expected that designs with re-entrant VT gas flow, or with solid rather than open inserts, would lead to smaller gradients, but such factors seem to have relatively little influence. It is tempting to speculate on further probe design and/or sample features that could reduce gradients, such as metal VT gas inlet ducts/frits, sapphire inserts, thermal insulation between insert and supports, capillary versus annular samples, and concentric solid sapphire inserts, but such work is beyond the scope of this paper.

Acknowledgments

Support from Syngenta UK Ltd. is gratefully acknowledged. This work was funded by the Engineering and Physical Sciences Research Council (Industrial CASE studentship number 11440208 to IS and grant number EP/H024336).

Appendix A. Analytical expression for the velocity spectrum $M(v)$

Eq. (5) for the spatial dependence of convective flow driven by a horizontal temperature gradient can be rewritten using Eq. (6), assuming conductive cylinder walls as discussed above, as

$$v(r',\phi) = v_{max}\frac{3\sqrt{3}}{2}r'[1-r'^2]\cos(\phi) = \alpha r'[1-r'^2]\cos(\phi) \tag{A1}$$

where r' is the dimensionless radius r/R and

$$\alpha = \frac{3\sqrt{3}}{2}v_{max} = \frac{R^3 g\beta\rho}{4\eta}\frac{dT}{dx} \tag{A2}$$

Dropping the primes on r and v for convenience, the velocity spectrum becomes

$$M(v) = LM_{vol}R^2\int_0^1\int_0^{2\pi}\delta(\alpha r[1-r^2]\cos\phi - v)r\,d\phi\,dr \tag{A3}$$

Using the integral form of the δ function gives

$$M(v) = LM_{vol}R^2\int_{-\infty}^{\infty}\int_0^1\int_0^{2\pi}re^{ikv-ik\alpha r[1-r^2]\cos\phi}d\phi\,dr\,dv \tag{A4}$$

in which it is convenient to choose as conjugate variable

$$k = \gamma G\delta\Delta \tag{A5}$$

Integrating over ϕ gives (see Ref. [30] p. 360, 9.1.21)

$$M(v) = LM_0R^2\int_{-\infty}^{\infty}\int_0^1 e^{ikv}rJ_0(k\alpha r[1-r^2])dr\,dk \tag{A6}$$

where J_0 is the Bessel function of the first kind. The convenience of (A4) then becomes apparent; the signal attenuation $S(\Delta\Delta)$ reduces to

$$S(\Delta\Delta) = 2\int_0^1 rJ_0(k\alpha r[1-r^2])dr \tag{A7}$$

Returning to $M(v)$, using a standard integral (see Ref. [30] p. 487, 11.4.37) and making the substitution $x = r^2$ yields

$$M(v) = LM_{vol}\frac{R^2}{\alpha}\int_{x_{min}}^{x_{max}}\frac{1}{\sqrt{\alpha^2x(1-x)^2 - v^2}}dx \tag{A8}$$

where the integration limits confine integration to the region where the integrand is real and $x_{min} < x_{max} < x_r$ are the three (real) roots of the cubic

$$x^3 - 2x^2 + x - \left(\frac{v}{\alpha}\right)^2 = 0 \tag{A9}$$

A further standard integral (Ref. [29], p. 597, 17.4.62) then finally gives

$$M(v) = LM_{vol}\frac{2R^2}{\alpha\sqrt{x_r - x_{min}}}K\left(\frac{x_{max}-x_{min}}{x_r-x_{min}}\right) \tag{A10}$$

where $K(q)$ is the complete elliptic integral of the first kind. Substituting in the real roots of the cubic in trigonometric form

$$\begin{aligned} x_r &= \frac{2}{3}\left[1+\left\{\cos\left(\frac{\theta_V}{3}\right)\right\}\right];\\ x_{max} &= \frac{2}{3}\left[1+\left\{\cos\left(\frac{\theta_V-2\pi}{3}\right)\right\}\right];\\ x_{min} &= \frac{2}{3}\left[1+\left\{\cos\left(\frac{\theta_V-4\pi}{3}\right)\right\}\right] \end{aligned} \tag{A11}$$

where

$$\theta_V = \arccos\left(\frac{27v^2}{2\alpha^2}-1\right) \tag{A12}$$

finally gives

$$M(v) = LM_{vol}\frac{\sqrt[4]{12}R^2}{\alpha\sqrt{\sin\left(\frac{\theta_V+\pi}{3}\right)}}K\left(\frac{\sin\left(\frac{\theta_V}{3}\right)}{\sin\left(\frac{\theta_V+\pi}{3}\right)}\right) \tag{A13}$$

for the range $v_{min} \leqslant v \leqslant v_{max}$.

References

[1] M. Lappa, Thermal Convection: Patterns, Evolution and Stability, John Wiley & Sons, 2009.
[2] G.A. Ostroumov, Svobodnaya convectzia v ousloviakh vnoutrennei zadachi, Gosud. Izd. Techn-Teor. Lit. (translation available at <https://archive.org/details/nasa_techdoc_20030068786>), 1952.
[3] N.M. Loening, J. Keeler, Measurement of convection and temperature profiles in liquid samples, J. Magn. Reson. 139 (1999) 334–341.
[4] N. Hedin, I. Furó, Temperature imaging by H-1 NMR and suppression of convection in NMR probes, J. Magn. Reson. 131 (1998) 126–130.
[5] K.C. Chung, H.Y. Yu, S. Ahn, Convection effects on PGSE-NMR self-diffusion measurements at low temperature: investigation into sources of induced convective flows, Bull. Korean Chem. Soc. 32 (2011) 1970–1974.
[6] M. Nilsson, G.A. Morris, Improving pulse sequences for 3D DOSY: convection compensation, J. Magn. Reson. 177 (2005) 203–211.
[7] E. Martinez-Viviente, P.S. Pregosin, Low temperature H-1-, F-19-, and P-31-PGSE diffusion measurements. Applications to cationic alcohol complexes, Helv. Chim. Acta 86 (2003) 2364–2378.
[8] W.J. Goux, L.A. Verkruyse, S.J. Salter, The impact of Rayleigh–Benard convection on NMR pulsed-field-gradient diffusion measurements, J. Magn. Reson. 88 (1990) 609–614.
[9] N. Esturau, F. Sanchez-Ferrando, J.A. Gavin, C. Roumestand, M.A. Delsuc, T. Parella, The use of sample rotation for minimizing convection effects in self-diffusion NMR measurements, J. Magn. Reson. 153 (2001) 48–55.
[10] J. Lounila, K. Oikarinen, P. Ingman, J. Jokisaari, Effects of thermal convection on NMR and their elimination by sample rotation, J. Magn. Reson., Ser. A 118 (1996) 50–54.
[11] K. Hayamizu, W.S. Price, A new type of sample tube for reducing convection effects in PGSE-NMR measurements of self-diffusion coefficients of liquid samples, J. Magn. Reson. 167 (2004) 328–333.
[12] M.A. Connell, P.J. Bowyer, P.A. Bone, A.L. Davis, A.G. Swanson, M. Nilsson, G.A. Morris, Improving the accuracy of pulsed field gradient NMR diffusion experiments: correction for gradient non-uniformity, J. Magn. Reson. 198 (2009) 121–131.
[13] W.S. Price, H. Ide, Y. Arata, Translational and rotational motion of isolated water molecules in nitromethane studied using 17O NMR, J. Chem. Phys. 113 (2000) 3686–3689.
[14] A. Jerschow, N. Müller, Suppression of convection artifacts in stimulated-echo diffusion experiments. Double-stimulated-echo experiments, J. Magn. Reson. 125 (1997) 372–375.
[15] A. Jerschow, N. Müller, Convection compensation in gradient enhanced nuclear magnetic resonance spectroscopy, J. Magn. Reson. 132 (1998) 13–18.
[16] G.H. Sørland, J.G. Seland, J. Krane, H.W. Anthonsen, Improved convection compensating pulsed field gradient spin-echo and stimulated-echo methods, J. Magn. Reson. 142 (2000) 323–325.
[17] X. Zhang, C.G. Li, C.H. Ye, M.L. Liu, Determination of molecular self-diffusion coefficient using multiple spin-echo NMR spectroscopy with removal of convection and background gradient artifacts, Anal. Chem. 73 (2001) 3528–3534.
[18] M. Nilsson, A.M. Gil, I. Delgadillo, G.A. Morris, Improving pulse sequences for 3D diffusion-ordered NMR spectroscopy: 2DJ-IDOSY, Anal. Chem. 76 (2004) 5418–5422.
[19] M.J. Stchedroff, A.M. Kenwright, G.A. Morris, M. Nilsson, R.K. Harris, 2D and 3D DOSY methods for studying mixtures of oligomeric dimethylsiloxanes, Phys. Chem. Chem. Phys. 6 (2004) 3221–3227.
[20] K.I. Momot, P.W. Kuchel, Convection-compensating diffusion experiments with phase-sensitive double-quantum filtering, J. Magn. Reson. 174 (2005) 229–236.
[21] G. Zheng, W.S. Price, Simultaneous convection compensation and solvent suppression in biomolecular NMR diffusion experiments, J. Biomol. NMR 45 (2009) 295–299.
[22] A. Jerschow, Thermal convection currents in NMR: flow profiles and implications for coherence pathway selection, J. Magn. Reson. 145 (2000) 125–131.
[23] A. Gibbs, G.A. Morris, A.G. Swanson, D. Cowburn, Suppression of t1 noise in 2D NMR spectroscopy by reference deconvolution, J. Magn. Reson., Ser. A 101 (1993) 351–356.
[24] E.O. Stejskal, J.E. Tanner, Spin diffusion measurements: spin echoes in the presence of a time-dependent field gradient, J. Chem. Phys. 42 (1965) 288.
[25] Q. He, Z. Wei, Convection compensated electrophoretic NMR, J. Magn. Reson. 150 (2001) 126–131.
[26] W.M. Haynes, CRC Handbook of Chemistry and Physics: A Ready-reference Book of Chemical and Physical Data, CRC Press, Boca Raton, FL, 2014.
[27] N. Hedin, I. Furó, Temperature imaging by H-1 NMR and suppression of convection in NMR probes, J. Magn. Reson. 131 (1998) 126–130.
[28] A.E. Derome, M.P. Williamson, Rapid-pulsing artifacts in double-quantum-filtered cosy, J. Magn. Reson. 88 (1990) 177–185.
[29] P.W.A. Howe, Rapid pulsing artefacts in pulsed-field gradient double-quantum filtered COSY spectra, Magn. Reson. Chem. 52 (2014) 329–332.
[30] M. Abramowitz, I.A. Stegun, Handbook of Mathematical Functions, N.B.S. Applied Mathematics Series, vol. 55, 10th printing, US Government Printing Office, Washington DC, 1972.